SPE 110219

A New Thermal Compositional Reservoir Simulator with a Novel "Equation Lineup" Method

C.K. Huang, Y.K. Yang*, M.D. Deo, University of Utah

This paper was prepared for presentation at the 2007 SPE Annual Technical Conference and Exhibition held in Anaheim, California, U.S.A., 11–14 November 2007.

Abstract

In a thermal-compositional reservoir simulator, pressures, saturations, temperature and compositions in all the existing phases must be solved. When this equation system is solved implicitly, a system of nonlinear equations results, which is solved by the Newton's method. This requires computation of the Jacobian matrix of partial derivatives. If the appropriate dependent variable is not lined-up with the correct equation, zero pivot elements are generated in the Jacobian matrix. This situation is complicated by the fact that new phases may appear, and existing phases may disappear leading to the type and number of dependent variables changing constantly. Elimination of these zero pivot elements using pivoting is computationally expensive for large matrix systems. In this paper, we present a robust algorithm for lining-up the dependent variables and the equation system appropriately to avoid zero pivots in the Jacobian.

This technique can be applied to the thermal-compositional model with any number of components and phases and there is no constraint on the number of thermal equilibrium relationships. In a system with Nc components and Np phases, and Ne thermal equilibrium constraints, Nc+Np+Ne+2 dependent variables are lined with appropriate equations (pressure and temperature are the two additional variables). Any phase equilibrium calculation (K-value based, equation of state) can be used in this approach.

The motivation for equation line-up and some previous methods are presented followed by a description of the conservation and constraint equations in thermal modeling. A brief description of the simulator framework that allows coupling different physical models and discretization methods is provided. The rules of variable selection for avoiding zero pivots are discussed in detail, including a method to obtain analytical derivatives. As proof of concept, two applications are discussed: a steamflooding example in a fractured system, using the discrete-fracure modeling approach and in situ combustion. A control volume finite-element discretization is used in steamflooding while a finite-difference approach based on the Cartesian grid is employed in the in situ combustion application.

Introduction

Reservoir simulation requires solutions of nonlinear partial differential equations. The set of nonlinear equations that result when the differential equations are discretized are solved using the Newton's method, when an implicit solution procedure is employed.

Among reservoir simulators, thermal simulators are the most complex. Solution of an energy balance equation is required along with component conservation equations. Pressures and saturations are additional variables. Writing a general thermal simulator, where phases appear and disappear, and where components get converted to new products, requires a general and robust approach for selecting how dependent variables get lined up for solution alongside the Jacobian matrix. If proper alignment is not achieved, zero pivot elements result and to overcome this, computationally expensive pivoting is necessary. Different variable alignment approaches have been proposed previously. Commonly used strategies for lining up variables with equations are summarized below. The vector $\vec{v}$ refers to the dependent variables, while the vector $\vec{R}$ points to the equations to be solved.

Coats et. al.[1]:

$$\vec{v} = v\{S_1, ..., S_{Np-1}, P, X_{Np+1}, ..., T\}$$

$$\vec{R} = R\{R_1, ..., R_{Nc}, R_E\}$$

Where, variable X_i's represent the mole fraction of component 'i' in its "master phase". The mole fraction of component 'i' in phase p ($x_{p,i}$'s) can be calculated by $x_{p,i} = K_{i,p} X_i$. S_j is replaced by X_j if phase 'j' is absent. Mass conservation equation for the coke component is considered as a constraint equation.

* Now at Terra Tek, a Schlumberger Company

Eclipes 300[2]:

$$\vec{v} = v\{m_1, ..., m_{Nc-1}, m_w, E, P\}$$

$$\vec{R} = R\{R_1, ..., R_{Nc-1}, R_w, R_E, R_V\}$$

Where R_E is the total internal energy and R_V is the volume constraint equation computed by $R_V = V_{pore} - V_{fluid} = 0$. With this approach, variables do not have to be realigned upon phase changes.

CMG(SXY option) STARS[3]:

$$\vec{v} = v\{P, S_o, ..., x_{oc}, S_g y_{NCG_1}, ..., S_g y_{NCG_{ncg}}, C_{s_1}, ..., C_{s_{ns}}, T\}$$

$$\vec{R} = R\{R_w, R_{o_1}, ..., R_{o_{oc}}, ..., R_{NCG_1}, ..., R_{NCG_{ncg}}, R_{s_1} ..., R_{s_{ns}}, R_E\}$$

The gas molar constraint or the volume constraint is solved optionally depending on the flash algorithm and the equilibrium condition. For a wide-boiling system, the saturation constraint is used while the gas phase constraint is used in a narrow-boiling system. A series of rules are required to re-align equations and variables once phase change occurs.

Chen et. al. [4]:

$$\vec{v} = v\{x_1, ...x_{Nc-2}, P, S_w, S_g\}$$

$$\vec{R} = R\{R_1, ...R_{Nc-1}, R_w, R_E\}$$

In this case, $x_i = \sum_{p=1}^{Np} x_{p,i}$ is solved. S_g is replaced by T if the block is unsaturated.

Buchanan et. al. [5]:

$$\vec{v} = v\{P, z_2, ...z_{Nc}, T, F_g\}$$

$$\vec{R} = R\{R_w, R_2, ..., R_{Nc}, R_E, R_F\}$$

Where, R_F is the flash constraint and is aligned with gas fraction F_g. The approach required no re-alignment in phase changes.

Grabowski et. al. [6]:

$$\vec{v} = v\{P, S_w, S_o, T, x_{g,Ng}, x_{g,No+2}, x_{g,Ng-1}, x_{o,2}, ...x_{o,No-1}\}$$

$$\vec{R} = R\{R_w, R_2, ..., R_{Nc01}, R_E\}$$

The model could consider only one solid component (coke), and the coke conservation equation is solved explicitly.

Rubin et. al. [7]:

Equation re-combination was required in this approach. The existence of non-condensible gas demanded a different algorithm to align the variables. Phase change also required variable re-alignment.

It is not convenient to implement analytical Jacobian using the techniques described previously. One of the primary motivations for developing the alignmentl procedure in this work was to be able to compute analytical Jacobian matrices. The thermal simulator described in this paper was developed under the UFES (Utah Finite Element Simulator) modular framework. The oil reservoir simulator development in UFES is divided into two main modules: PhyiscalModel (PM) and DiscretizationMethod (DM). The DM module is responsible for computing the driving forces term $-\mathbf{k}\nabla\Phi$ for each flux so it is a discrete-method dependent module. The focus of this paper is on the development of the thermal model in PM which controls the computation of the physical/chemical properties and the solution of the governing equations.

The key features of this thermal model enumerated below.

1. P, S_p, $x_{p,\,i}$ and T are used as variables and a novel alignment approach is proposed to prevent the occurrence of zero pivots in the Jacobian matrix.
2. Equation decoupling is used to separate the solution sequence of conservation equations and constraint equations.
3. The number of components is a variable and is determined in input data. The components are allowed to be distributed in the oil, gas, water and solid phases depending on the component-phase distribution table.
4. The pore volume is occupied by oil, gas, water, solid phases (consisting of active solid components), and the inert components are considered to be part of the rock matrix.
5. The number and types of chemical reactions are determined in the input data file.
6. Concentration driven diffusion is assumed negligible.
7. The model is solved fully implicitly. The Jacobian matrix is computed analytically to improve the efficiency of the Newton's method.

The first three features generalize the mass conservation of the fluid and non-fluid components, and provide a flexible handle for solving the mass conservation equations. The last feature provides a high accuracy “searching slope” for Newton's method. The computation of analytical expressions for the Jacobian derivatives can easily be achieved because of the modularized design.The simulator can be used on applications such as steam flooding, in-situ conversion, and in-situ combustion. After minor modifications, the simulator can be extended to other applications such as polymer flooding and CO_2 sequestration.

In this paper, we emphasize the introduction of the solution procedure of the thermal model including the new equation line-up method, computation of the analytical Jacobian matrix and equation decoupling. Two applications, steam flooding in an unstructured grid domain and in-situ combustion in the Cartesian domain, are used to show the adaptability of this new model.

Mathematic model

Governing equations

For an Nc component and Np phase thermal recovery problem, there are Nc + 1 conservation equations to be solved: Nc mass balance equations and one energy balance equation.

The mass balance equation of component 'i' is given by

$$\sum_{p=1}^{Np} x_{p,i}\rho_p \nabla\cdot\vec{f}_p + q_i + \sum_{r=1}^{Nr} \Re_{r,i} = \frac{\partial}{\partial t}\phi \sum_{p=1}^{Np} x_{p,i} S_p \rho_p$$

For the reaction term, rate expressions of the power-law type $\Re_{r,i} = \mathbf{a_{r,i}} k_r \prod_{j=1}^{Nc} C_j^{n_j}$ are used.

The energy balance equation is written as:

$$\sum_{p=1}^{Np} H_p \rho_p \nabla\cdot\vec{f}_p + \nabla\cdot\mathbf{k_c}\nabla T + Q_w + Q_{loss} =$$

$$\frac{\partial}{\partial t}\phi \sum_{p=1}^{Np} U_p S_p \rho_p + (1-\phi)\overline{U}_R$$

The heat of reaction does not appear explicitly in the energy balance equation. The enthalpy differences in the reactant and product streams automatically account for the heats of reaction [9]. The heat of reaction has to be specified only if all reference enthalpies are zero.

In mass and energy conservation equations, the volumatric flux $\vec{f}_p$ for phase 'p' is computed by Darcy's flow equation

$$\vec{f}_p = -\mathbf{k}\frac{kr_p}{\mu_p}(\nabla P_p + \gamma_p \nabla z)$$

For such a system, we can define the volume constraint

$$\sum_{p=1}^{Np} S_p = 1,$$

and Np phase constraints

$$\sum_{i=1}^{Nc} x_{p,i} = 1.$$

The number of the equilibrium constraint equations depends on the the number of equilibrium relationships defined by the user. There is a K-value equation for each component that partitions between two different phases.

$$\frac{x_{p_L,i}}{x_{pH,i}} = K_{i,p_L,p_H}$$

The implicit form to represent all the conservation equations and constraint equations can be written as

$$R_{Ci} = R_{Ci}(P, S_p, x_{p,i}, T)$$

$$R_E = R_E(P, S_p, x_{p,i}, T)$$

$$R_{\Sigma S} = R_{\Sigma S}(S_p)$$

$$R_{\Sigma x} = R_{\Sigma x}(x_{p,i})$$

$$R_{Kk} = R_{Kk}(P, x_{p,i}, T)$$

In above equation set, $i \in [1, Nc]$, $p \in [1, Np]$ and $k \in [1, Ne]$. The equations to compute the properties in each equation are summarized in the Appendix.

Well models

Volumetric flow of phase 'p' between the well node and control-volume 'ι' can be computed by

$$q_{p,\iota} = PI_\iota \xi_p (P_{wb} - P_{p,\iota})$$

For production well, $\xi_p = \frac{kr_p}{\mu_p}$ is the relative mobility for phase 'p' computed based on the condition of the production block. For the injection well, total mobility $\xi_T = \sum_{p=1}^{Np} \frac{kr_p}{\mu_p}$ is used.. The well index PI_ι is generally computed by

$$PI_\iota = \frac{2\pi h k_{\perp w} f_h f}{\ln\frac{r_e}{r_{wb}} + S}$$

In the Cartesian grid, r_e is computed by

$$r_e = \frac{2\,geofac}{\sqrt{\pi}} \frac{\sqrt{\sqrt{k_{yy}/k_{xx}}(\Delta x)^2 + \sqrt{k_{xx}/k_{yy}}(\Delta y)^2}}{(k_{yy}/k_{xx})^{1/4} + (k_{xx}/k_{yy})^{1/4}}$$

For the unstructured grid, one option to compute r_e is

$$r_e = \left[V_\iota \frac{3}{4\pi}\right]^{1/3}$$

V_ι is the volume of the control-volume 'ι'where the well is completed. This option has been implemented in the Control Volume Finite Element (CVFE) model discussed later in the paper.

Heat loss models

Vinsome et. at.[10] suggest a semi-analytical model to compute the heat loss to the surrounding rock. The model requires no information from interal gridding so it is directly

implemented without any modification in both the Cartesian grid and the unstructured grid model.

Solution procedure and variable alignment

The variables $\vec{v} = \{P, S_p, x_{p,i}, T\}$ in the non-linear equation set are updated by $\vec{v}^{t+1} = \vec{v}^{t} + \delta\vec{v}$ at each new time step where $\delta\vec{v}$ is computed by the Newton's method.

$$\vec{R} = -\left[\frac{\partial R}{\partial v}\right]\delta\vec{v}$$

Analytical Jacobian derivatives $\left[\frac{\partial R}{\partial v}\right]$ are usually computed by applying a series of chain rules.

$$\frac{\partial R}{\partial v} = \frac{\partial R}{\partial P}\frac{\partial P}{\partial v} + \frac{\partial R}{\partial T}\frac{\partial T}{\partial v} + \sum_{p=1}^{Np}\left(\frac{\partial R}{\partial S_p}\frac{\partial S_p}{\partial v} + \sum_{i=1}^{Nc}\frac{\partial R}{\partial x_{p,i}}\frac{\partial x_{p,i}}{\partial v}\right)$$

$\frac{\partial P}{\partial v}$, $\frac{\partial S_p}{\partial v}$, $\frac{\partial x_{p,i}}{\partial v}$, $\frac{\partial T}{\partial v}$ are called unit derivatives which are either unity or zero. The derivatives of phase pressure require special care and are explained in the Appendix.

Zero pivots in the Jacobian matrix make it singular and must be avoided. The strategy to make this happen is to align each variable to the equation which is a function of that variable. For example, the volume constraint equation $R_{\sum S}$ can only be aligned to S_p. Aligning $R_{\sum S}$ to any variable other than S_p causes the derivative $\left.\frac{\partial R_{\sum S}}{\partial v}\right|_{v \neq S_p} = 0$.

The equations and the variables are aligned using a series of rules. As a result, the Jacobian matrix does not contain any zero pivots.

The residual function vector $\vec{R}$ is organized in the following order.

1. Component mass conservation equations (oleic components, gaseous components, aqueous components, solid components)
2. Energy conservation equation
3. Volume constraint equation
4. Phase constraints (oil, gas, water, solid)
5. Thermal equilibrium constraints (oleic components, gaseous components, aqueous components, solid components)

A generalized component numbering scheme is shown in Table 1. Also shown in this table is the way components partition between the different (four) phases.

After the order of the residual functions is decided, the equations are aligned with the variables by observing the following algorithm:

1. Do no solve $R_{\sum S}$ if only one phase exists.
2. Do not solve R_{Kk} if the component or the phase does not exist.
3. Do not solve R_{Ci} if component 'i' does not exist.
4. Align the first available S_P to $R_{\sum S}$.
5. $R_{\sum x}$'s are aligned with available $x_{p,i}$. While doing this, 'p' = 'i' condition get higher priority. For example, $x_{1,1}$ is aligned with the $R_{\sum x1}$.
6. R_{Kk}'s are aligned with available $x_{p,i}$ (align 'i' index, if no $x_{p,i}$ is available, using T as the dependent variable).
7. Align remaining $x_{p,i}$ to R_{Ci} based on the i index.
8. Align remaining S_p to not-yet-aligned R_{Ci} (check if component 'i' exists in phase 'p'). If R_{Ci}'s are not available, use the R_E.
9. Align P to remaining R_{Ci}'s.
10. If T is still available, align it with the R_E.

In each iteration step, phase change is handled by the following procedure.

For $S_p < 0$.:

Phase 'p' disappears, S_p and all corresponding $x_{p,I}$'s are set to zero.

For $S_p = 0$.:

$\sum_{i=1}^{Nc} x_{p,i}$ is monitored. Once the summation is ≥ 1, the phase reappears. A small initial guess, for example, (10^{-6}) is set to S_p and all corresponding $x_{p,i}$'s are updated according to the results from the flash calculation.

The Jacobian matrix is populated in sub-blocks as shown.

$$\begin{pmatrix} R_{\boldsymbol{p}} \\ R_{\boldsymbol{s}} \end{pmatrix}_I = -\begin{bmatrix} A & B \\ C & D \end{bmatrix}_{I,I}\begin{pmatrix} \delta v_{\boldsymbol{p}} \\ \delta v_{\boldsymbol{s}} \end{pmatrix}_I + \sum_J -\begin{bmatrix} A & B \\ C & D \end{bmatrix}_{I,J}\begin{pmatrix} \delta v_{\boldsymbol{p}} \\ \delta v_{\boldsymbol{s}} \end{pmatrix}_J$$

where A, B, C and D represent $\frac{\partial R_{\boldsymbol{p}}}{\partial v_{\boldsymbol{p}}}$, $\frac{\partial R_{\boldsymbol{p}}}{\partial v_{\boldsymbol{s}}}$, $\frac{\partial R_{\boldsymbol{s}}}{\partial v_{\boldsymbol{p}}}$ and $\frac{\partial R_{\boldsymbol{s}}}{\partial v_{\boldsymbol{s}}}$, respectively. The subscripts $_{\boldsymbol{p}}$ and $_{\boldsymbol{s}}$ represent primary (conservation) and secondary (constraint), equations respectively. Sub-block C and D are located only on the diagonal; therefore, this system can be decoupled by the

Gaussian elimination technique. After the decoupling, the primary part and the secondary part can be solved separately.

$$-\left(R_{\rho I}-\sum_J B_{I,J}D_I^{-1}R_{sI}\right)=\left[A_I-B_ID_I^{-1}C_I\right]\left(\delta v_{\rho I}\right)$$
$$+\sum_J\left[A_{I,J}-B_{I,J}D_I^{-1}C_I\right]\left(\delta v_{\rho J}\right)$$
$$\left(\delta v_{sJ}\right)=-D_I^{-1}\left(C_I\left(\delta v_{\rho I}\right)+R_{sI}\right)$$

The computation becomes more efficient since a smaller system (primary part) is solved by the linear solver.

The GMRES iterative solver was used for all the cases in this paper. The solver and ILU preconditioner were provided by AztecOO package in the Trilinos project.

Applications

Steam flooding

Steam flooding simulation was performed with the discrete fracture reservoir model (DFM) shown in Figure 1 with explicit fracture representation. The model consists of 5868 nodes, 28469 tetrahedral elements for representing the matrix and 3355 triangular elements for fractures. The model considered three components: heavy oil, light oil and water. The component distribution in this model is shown in Table 2 and data related to this model are given in Table 3. There were two sets of fractures in the simulation domain; one in the north-south direction and other in the east-west direction. A full scale inverted nine-spot (injection well at the center surrounded by eight producers) scheme was modeled. The impact of two different fracture/matrix permeability contrasts (2 and 100) on oil production was examined. The injection well and three production wells P3, P4 and P6 were located on fractures (see Figure 1).

Results of temperature, saturations of oil and water on 2000^{th} day for the high permeability contrast and the low permeability contrast are shown in Figures 2, 3 and 4. The oil was completely expelled from the swept zone. In the low constrast case, the swept zone is nearly uniform in every direction since the fractures do not have a significant impact. In high contrast case, the permeability of fracture is significantly larger compared with the matrix. Therefore, the flow is dominated by the fracture network. The production rates in P3, P4 and P6 are higher (see the oil production rate in Figure 5 and water saturation in Figure 4 b) and the breakthrough times are earlier.

In-situ combustion

Thermal module was integrated with the Cartesian coordinate finite difference DM module for modeling a quarter size of a five-spot in-situ combustion process. A $10 \times 10 \times 5$ grid shown in Figure 6 (10 ft × 10 ft × 5ft for each block) was used to simulate a thick, uniform formation containing heavy oil, light oil, water and coke. The air was injected at one corner and oil is produced at the opposite corner. Both the wells were completed in the bottom layer. Four chemical reactions were considered in this model. CO_2 and N_2 were lumped together as one inert gas component. The component phase distribution is shown in Table 4 and the data related to this model are given in Table 5. The gas components can dissolve into the oil phase. Coke component existed originally and can either be regenerated by cracking reaction from heavy oil or be consumed in coke oxidation reaction. The blocks around the injection well were set to 800 R initially to simulate the ignition. Dry injection and varied amounts of water co-injection were compared. Water-air co-injections were continued from 20^{th} to 25^{th} day. The heats of reactions were provided in the input data since the reference enthalpies for all the ncomponents were set to zero.

The results of temperature, oil and water saturations at the 40^{th} day are shown in Figures 7, 8 and 9. The average temperature is lower in the combusted zone in the water co-injection case because the water evaporated in this zone and carried the heat toward the production well. The water recondensted beyond the combustion front and released the latent heat to heat up the reservoir (see water recondensation in Figure 9). Therefore, the oil bank (see Figure 8) in water-coinjection had moved farther away from the combustion front. The increase in the oil production rate due to this phenomenon is observed in Figure 10 for the wet combustion cases.

Summary

The development of a fully implicit, general compositional thermal model using a new equation line-up concept was presented in this paper. The new equation line-up procedure allows for computations of analytical Jacobian matrices. A study of two different applications, one with the control-volume finite element discretization and the other with finite difference showed that a given physical model can be integrated with different "DiscretizationMethod" modules to solve the reservoir problem. Incorporation of a discrete-fracture representation provides an alternative to dual porosity models for simulating thermal recovery in fractured reservoirs. Possible applications include modeling naturally fractured reservoirs and hydraulically fractured wells.

Acknowledgements

Financial support from the U.S. DOE National Energy Technology Laboratory for the project Parallel, Multigrid, Finite-Element Simulator for Faulted/Fractured, and Other Complex Reservoirs Based on Common Component Architecture (CCA) (DE-FC26-04NT15531) is gratefully acknowledged. We would also like to thank Computer Modeling Group for providing an academic license for STARS which helped us compare and index the new simulator.

Nomenclature

Subscripts

°	Reference state
C_i	Index of residual function of conservation equation of component i
R	Rock
V	Index of residual function of volume constraint equation
E ,F	Index of residual function of energy conservation equation, flash constraint
o ,w ,g ,s ,l	Oil, water, gas, solid and liquid phase
p ,i ,r	Phase index, component index and reaction index
IG	Ideal gas
NCG_i	i^{th} non-condensible gas component
I, J	Control-volume index
ι	Layer index
Kk	Index of residual function of conservation equation of k_{th} thermal constraint equation
Ng ,No	Number of component in gas phase, oil phase
og ,op ,ow	Phase pair for oil and gas, oil and phase p, oil and water
P ,S	Primary and secondary
wb	Well bore
ΣS ,Σxp	Index of residual function of volume constraint and residual function of phase constraint of phase p

Symbols

c_p, c_{t_1}, c_{t_2}	Coefficient for molar density
cl_0, cl_1	Coefficient for liquid phase viscosity
cg_0, cg_1	Coefficient for gas phase viscosity
Cp_R, k_{Rcond}	Heat capacity, thermal conductivity of overburn/underburden
$\bar{C}p_{gi}$	The i^{th} heat capacity
$\vec{f}$	Volumetric flow rate
geofac, $k_{xx,yy,zz}$	Geology factor of the well, element of permeability tensor in different direction
$h, k_{\perp}, f_h, f, r_e, r_w, S$	Legth of well, permeability perpendicular to well, interval length factor, well fraction, effective radius, well radius, skin factor
$\bar{H}, \bar{U}, \overline{U}$	Molar enthalpy, molar internal energy, volumetric internal energy
H_{evp}, Ev	Coefficient for computing heat of evaporation
kr, kr_{ocw}, kr_{wc}	Relative permeability, oil relative permeability at ocnnate water, connate water relative permeability
kv_i	The i^{th} Coefficients for K equation
$K_{i,p1-p2}$	K-value of component I respect to phase p1 and p2
M	Molecular weight
Np, Nc, Ne, Nr	Number of phase, component, thermal equilibrium, reaction in the system
P, Pc, P_c	Pressure, critical pressure, capillary pressure
PI	Well index
q_i	Soruce/sink term of the conservation equation of the component i
S	Saturation
T, Tc	Temperature, critical temperature
v	Variable
X_i	Molar fraction of component i in its master phase
x	Molar fraction
x_i, y_i	Molar frction of component i in oil phase, gas phase
z_i	Global molar fraction of component i
α	Interaction factor in EOS
ϕ	Porosity
γ	Spacific density
μ	Viscosity
$\Re$	Chemical reaction term
ρ	Molar density
ξ	Volumetric mobility

References

1. K.H. Coats, “In-Situ Combustion Model, “Soc. Pet. Eng. J., pp. 533-554, 1980.
2. Eclips Simulaiton Software Manuals, Schlumberger, 2006.
3. CMG, Stars User’s Guide, 2006th ed., CMG, 150, 3553-31 Street N.W. Calgary, Alberta, Canada, October 2006.
4. Z. Chen, G. Huan, and B. Li, “Modeling 2D and 3D horizontal wells using CVFA,” Commun. Math. Sci., vol. 1, pp. 30-44, 2002.
5. W. L. Buchanan, “Simulating Steam Additive EOR Process,” Soc. Pet. Eng. J., pp. 255-265, 1985.
6. J. W. Grabowski, R. K. Vinsome, R. C. Line, A. Behie, and B. Rubin, “A fully implict general purpose finite-differnece thermal model for in situ combustion and steam,” Soc. Pet. Eng. J., pp.. 1-14, 1979.
7. B. Rubin and W. L. Buchanan, “A General Purpose Thermal Model,” Soc. Pet. Eng. J., pp. 202-216, 1985.
8. K. Aziz and A. Settari, Petroleum Reservoir Simulation. London: Applied Science Pulishers Ltd., 1979.
9. S. I. Sandler, Chemical and engineering thermodynamics. John Wiley & Sons, New York, 1989.
10. P. K. W. Vinsome and J. Westerveld, “A Simple Method for Predicting Cap and Base Rock Heat Losses in Thermal Reservoir Simulators,” J. Can. Pet. Tech., pp. 6-9, 1980.

Table 1: Numbering of components and their distribution in various phases

Component ID	Type	Oil	Gas	Water	Solid
Oleic phase Comps 1 to NO	Oleic	✓ | ✓	✓ | ✓		
Aq. phase Comps NO+1 to NO+NW	Aqueous		✓ | ✓	✓ | ✓	
Solid Phase Comps NO+NW+1 to NO+ NW+NS	Solid	(✓) | (✓)	(✓) | (✓)	(✓) | (✓)	✓ | ✓

Table 2: Component-phase partition in steam flooding

Component ID	Type	Oil	Gas	Water
Heavy oil	Oleic	✓	✓	
Light oil	Oleic	✓	✓	
Water	Aqueous		✓	✓

Table 3: Data used in the steamflood example

Fluid properties			
Prop.	Heavy oil	Light oil	H_2O
M (lb/lbmol)	675.0	156.7	18.0
Tc (R)	1597.4	1111.1	1165.1
Pc (psi)	120.0	305.0	3155.0
α	1.0	1.0	1.0
$\rho°$ (lbml/ft^3)	0.0914	0.3195	3.466
c_p (1/psi)	5.0e-6	5.0e-6	3.0e-6
c_{t_1} (1/R)	1.49e-4	2.84e-4	1.2e-4
c_{t_2} (1/R^2)	0.0	0.0	0.0
cl_0 (cP)	2.0e-7	5.0e-6	7.52e-3
cl_1 (R)	11260.0	7600.0	2492.75
cg_0 (cP)	3.93e-6	2.17e-6	8.82e-6
cg_1	1.102	0.943	1.116
$\Delta H°$ (Btu/lbmol)	0.0	0.0	0.0
ϵp_{g1} (Btu/lbmolR)	-8.14	-1.89	7.701
ϵp_{g2} (Btu/lbmolR^2)	0.549	0.1275	2.55e-4
ϵp_{g3} (Btu/lbmolR^3)	-1.68e-4	-3.9e-5	7.78e-7
ϵp_{g4} (Btu/lbmolR^4)	1.98e-9	4.6e-9	-0.15e-9
ΔH_{evp} (Btu/lbmolR^{Ev})	12198.0	1917.0	1657.0
Ev	0.38	0.38	0.38
kv_0 (psi)	1.55e5	8.334e8	1.72e6
kv_1 (1/psi)	0.0	0.0	0.0
kv_2	212.0	1.23e6	0.0
kv_3 (R)	-4.0e3	-1.6e4	-6869.59
kv_4 (R)	480.0	0.0	83.03

Rock properties, matrix				
$\phi°$	cr_p (1/psi)	$\overline{U}°_R$ (Btu/ft^3)	$k_{abs,matrix}$ (mD)	$k_{cond,matrix}$ (Btu/ftRD)
0.25	1.e-6	35.0	1.e2	35.0

Rock properties, fracture				
$\phi°$	cr_p (1/psi)	$\overline{U}°_R$ (Btu/ft^3)	$k_{abs,fractire}$ (mD)	$k_{cond,fracture}$ (Btu/ftRD)
0.25	1.e-6	35.0	(2.e2)[a] (1.e4)[b]	30.0

Rock-Fluid properties							
S_w	kr_w	kr_{ow}	P_{cow} (psi)	S_l	kr_g	kr_{og}	P_{cog} (psi)
0.218	0.000	0.545	-9.876	0.607	0.025	0.000	253.382
0.225	0.000	0.505	-9.782	0.940	0.002	0.000	39.071
0.236	0.000	0.465	-9.644	0.943	0.002	0.000	37.116
0.247	0.001	0.427	-9.506	0.946	0.002	0.001	35.159
0.258	0.001	0.389	-9.371	0.949	0.002	0.003	33.203
0.268	0.002	0.353	-9.233	0.955	0.001	0.012	29.302
0.278	0.003	0.318	-9.107	0.961	0.001	0.031	25.399
0.289	0.004	0.285	-8.969	0.964	0.001	0.046	23.444
0.300	0.005	0.252	-8.831	0.967	0.001	0.064	21.487
0.311	0.006	0.221	-8.697	0.970	0.001	0.088	19.530
0.333	0.009	0.164	-8.422	0.973	0.000	0.116	17.584
0.354	0.012	0.112	-8.157	0.976	0.000	0.149	15.629
0.364	0.014	0.089	-8.022	0.979	0.000	0.183	13.672
0.375	0.016	0.067	-7.884	0.982	0.000	0.220	11.716
0.386	0.018	0.048	-7.748	0.985	0.000	0.265	9.771
0.397	0.020	0.031	-7.612	0.988	0.000	0.311	7.815
0.407	0.022	0.017	-7.483	0.991	0.000	0.362	5.858
0.418	0.025	0.006	-7.348	0.994	0.000	0.419	3.901
0.429	0.027	0.000	-7.210	0.997	0.000	0.480	1.957
1.000	0.292	0.000	0.000	1.000	0.000	0.545	0.000

Initial conditions	
P (psi)	250.0
T (R)	565.0
z_{HO}	0.06
z_{LO}	0.04
z_{H_2O}	0.90

Well conditions		
	Producer	Injecitor
P (psi)	100.0	350.0
T (R)		892.0
Steam Qaul.		70.0%

Table 4: Component-phase partitioning in in-situ combustion

Component ID	Type	Oil	Gas	Water	Solid
Heavy oil	Oleic	✓	✓		
Light oil	Oleic	✓	✓		
CO_2+N_2	Oleic	✓	✓		
O_2	Oleic	✓	✓		
H_2O	Aqueous		✓	✓	
Coke	Solid				✓

Table 5: Property data in steaming flooding

Fluid properties						
Prop.	Heavy oil	Light oil	CO_2+N_2	O_2	H_2O	Coke
M (lb/lbmol)	675.0	156.7	40.8	32.0	18.0	13.0
Tc (R)	1597.4	1111.1	228.0	279.0	1165.1	
Pc (psi)	120.0	305.0	500.0	730.0	3155.0	
α	1.0	1.0	1.0	1.0	1.0	
$\rho°$ (lbml/ft^3)	0.0914	0.3195	1.4485	1.4485	3.466	4.4
c_p (1/psi)	5.0e-6	5.0e-6	0.0	0.0	3.0e-6	
c_{t_1} (1/R)	1.49e-4	2.84e-4	3.34e-6	3.37e-6	1.2e-4	
c_{t_2} (1/R^2)	0.0	0.0	0.0	0.0	0.0	
c_t (1/R)						0.0
c_{pt} (1/Rpsi)						0.0
cl_0 (cP)	4.02e-4	4.02e-4	1.88e-1	1.88e-1	7.52e-3	
cl_1 (R)	6121.6	6121.6	209.58	209.58	2492.75	
cg_0 (cP)	3.93e-6	2.17e-6	2.13e-4	2.20e-4	8.82e-6	
cg_1	1.102	0.943	0.702	0.721	1.116	
$\bar{H}°$ (Btu/lbmol)	0.0	0.0	0.0	0.0	0.0	0.0
$\bar{C}p_{g1}$ (Btu/lbmolR)	-8.14	-1.89	7.44	6.713	7.701	4.4
$\bar{C}p_{g2}$ (Btu/lbmolR^2)	0.549	0.1275	-0.0018	-4.88e-7	2.55e-4	0.0
$\bar{C}p_{g3}$ (Btu/lbmolR^3)	-1.68e-4	-3.9e-5	1.98e-6	1.29e-6	7.78e-7	0.0
$\bar{C}p_{g4}$ (Btu/lbmolR^4)	1.98e-9	4.6e-9	-4.78e-10	-4.78e-10	-0.15e-9	0.0
$\bar{H}_{evp}$ (Btu/lbmolR^{Ev})	12198.0	1917.0	991.0	482.0	1657.0	
Ev	0.38	0.38	0.38	0.38	0.38	
kv_0 (psi)	1.55e5	8.334e8	1.25e8	9.502e4	1.72e6	
kv_1 (1/psi)	0.0	0.0	0.0	0.0	0.0	
kv_2	212.0	1.23e6	0.0	0.0	0.0	
kv_3 (R)	-4.0e3	-1.6e4	-5586.1	-1322.19	-6869.59	
kv_4 (R)	480.0	0.0	0.29	11.61	83.03	

Chemical reacitons
$HO \rightarrow 2.154LO + 25.96Coke$ $rate = kC_{HO}$ Ea (Btu/lbmolR) = 27000.0; k_0 (1/D) = 1.e7; $\Delta\bar{H}$ (Btu/lbmol) = -40000.0; T_{act} (R) = 0.0
$LO + 14.06O_2 \rightarrow 11.96(CO_2 + N_2) + 6.58H_2O$ $rate = kC_{LO}P_{O_2}$ Ea (Btu/lbmolR) = 59450.0; k_0 (1/psiD) = 7.248e11; $\Delta\bar{H}$ (Btu/lbmol) = -2.9075e6; T_{act} (R) = 0.0
$HO + 60.55O_2 \rightarrow 51.53(CO_2 + N_2) + 28.34H_2O$ $rate = kC_{HO}P_{O_2}$ Ea (Btu/lbmolR) = 59450.0; k_0 (1/psiD) = 7.248e11; $\Delta\bar{H}$ (Btu/lbmol) = -1.252e7; T_{act} (R) = 950.0
$Coke + 1.18O_2 \rightarrow 1.00(CO_2 + N_2) + 0.55H_2O$ $rate = kC_{Coke}P_{O_2}$ Ea (Btu/lbmolR) = 25200.0; k_0 (1/psiD) = 10000.8; $\Delta\bar{H}$ (Btu/lbmol) = -2.25e5; T_{act} (R) = 0.0

Rock properties				
$\phi°$	cr_p (1/psi)	$\bar{U}°_R$ (Btu/ft^3)	k_{abs} (mD)	k_{cond} (Btu/ftRD)
0.25	0.0	35.0	1.e3	30.0

Over/under Burden properties	
Cp_R (Btu/ft^{3}R)	k_{Rcond} (Btu/ftRD)
35.0	24.0

Rock-Fluid properties							
S_w	kr_w	kr_{ow}	P_{cow} (psi)	S_l	kr_g	kr_{og}	P_{cog} (psi)
0.100	0.00	0.900	0.0	0.210	0.784	0.000	0.0
0.2500	0.004	.0600	0.0	0.320	0.448	0.010	0.0
0.440	0.024	0.280	0.0	0.400	0.288	0.024	0.0
0.560	0.072	0.144	0.0	0.472	0.184	0.052	0.0
0.672	0.168	0.048	0.0	0.580	0.086	0.152	0.0
0.752	0.256	0.000	0.0	0.680	0.024	0.272	0.0
1.000	1.000	0.000	0.0	0.832	0.006	0.448	0.0
				0.872	0.000	0.900	0.0
				1.000	0.000	0.900	0.0

Initial conditions	
P (psi)	2000.0
T (R)	610.0 (850.0)[a]
z_{HO}	0.085
z_{LO}	0.005
$z_{CO_2+N_2}$	0.0059
z_{O_2}	0.004
z_{H_2O}	0.9
z_{Coke}	0.0001

Well conditions			
	Producer	Injector	
		Dry	Wet[b]
P (psi)	1980.0	2200.0	2200.0
T (R)		650.0	650.0
x_{g,CO_2+N_2}		0.79	0.786
x_{g,O_2}		0.21	0.2093
x_{g,H_2O}			0.0047
$\frac{\text{Gas}}{\text{Water}}$ (vol. ratio)			$\frac{99.0}{1.0}, \frac{98.0}{2.0}, \frac{85.0}{15.0}, \frac{80.0}{20.0}$

[a]: ignition zone
[b]: water co-injeciton begins between 20-25[th] days

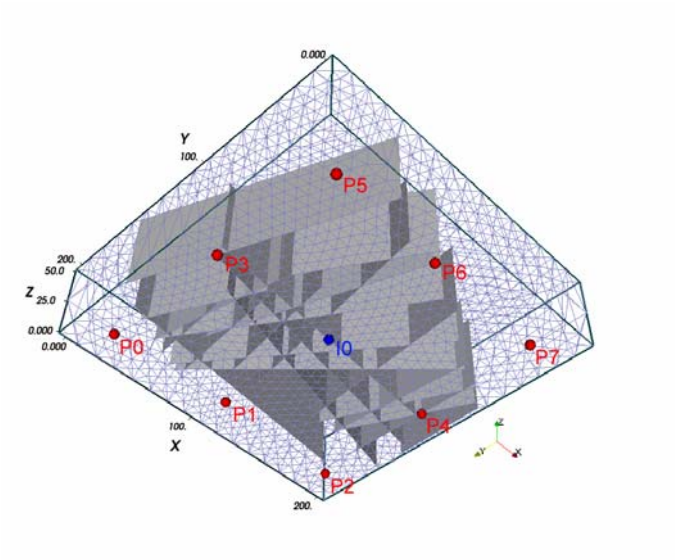

Figure 1: Steam flooding in an invertred nine-spot pattern in a fractured reservoir. Blue dot: injection well, red dots: production wells.

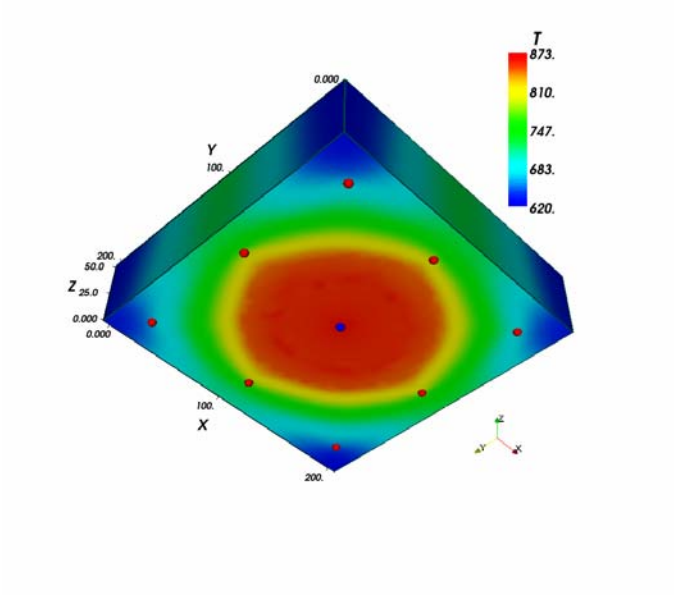

(a)

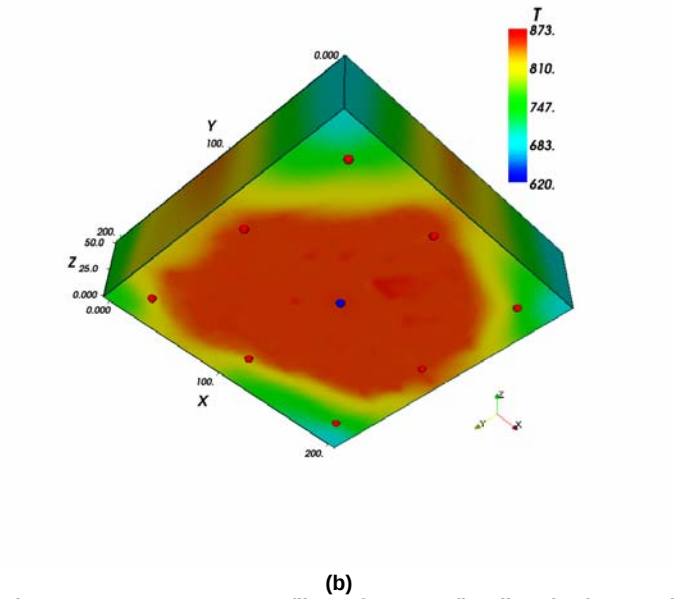

(b)

Figure 2: Temperature profiles of steam flooding in fractured reservoir (time = 2000 days). a. Fracture-matrix permeability contrast = 2; b. Fracture-matrix permeability contrast = 100

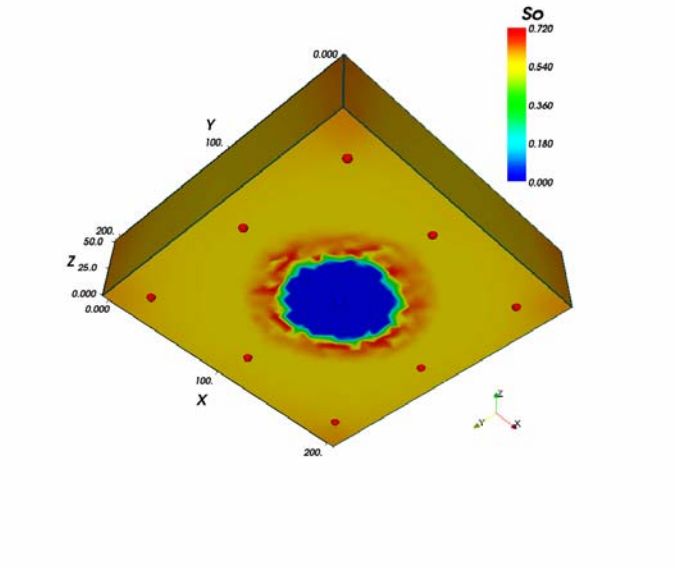

(a)

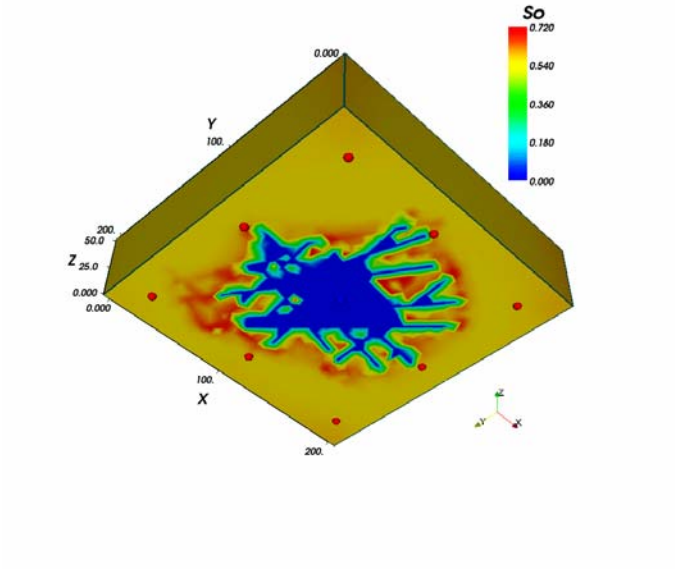

(b)

Figure 3: Oil saturation profiles of steam flooding in fractured reservoir (time = 2000 days). a. Fracture-matrix permeability contrast = 2; b. Fracture-matrix permeability contrast = 100

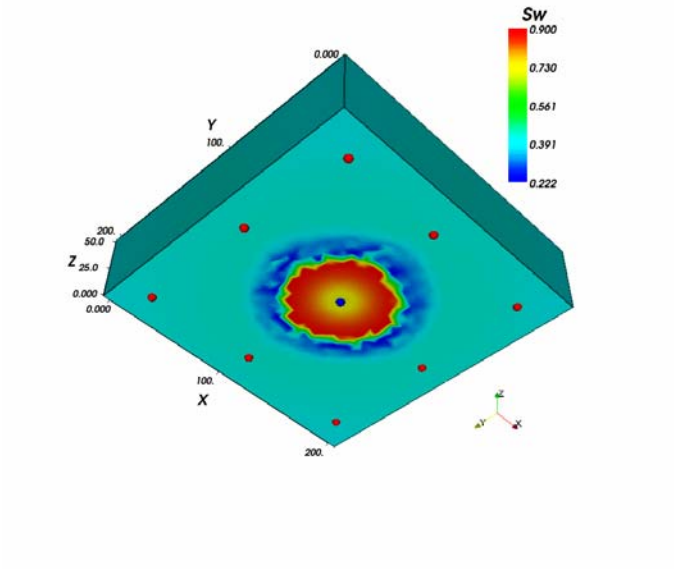

(a)

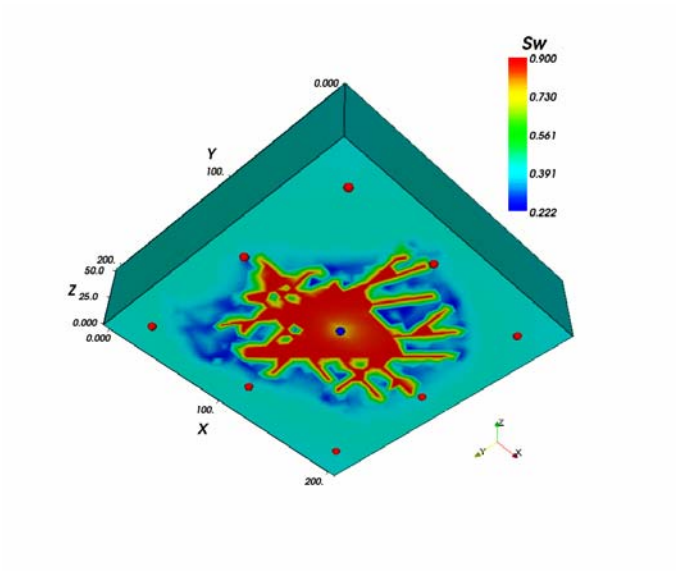

(b)

Figure 4: Temperature profiles of steam flooding in fractured reservoir (time = 2000 days). a. Fracture-matrix permeability contrast = 2; b. Fracture-matrix permeability contrast = 100

(b)

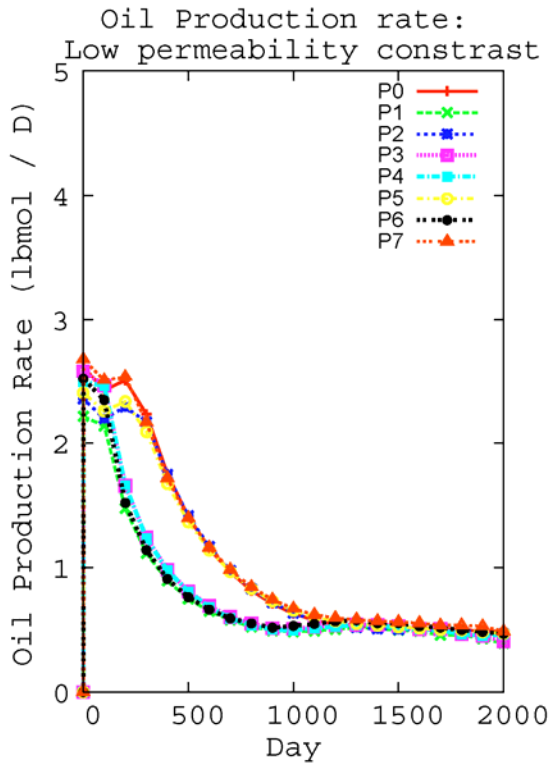

(a)

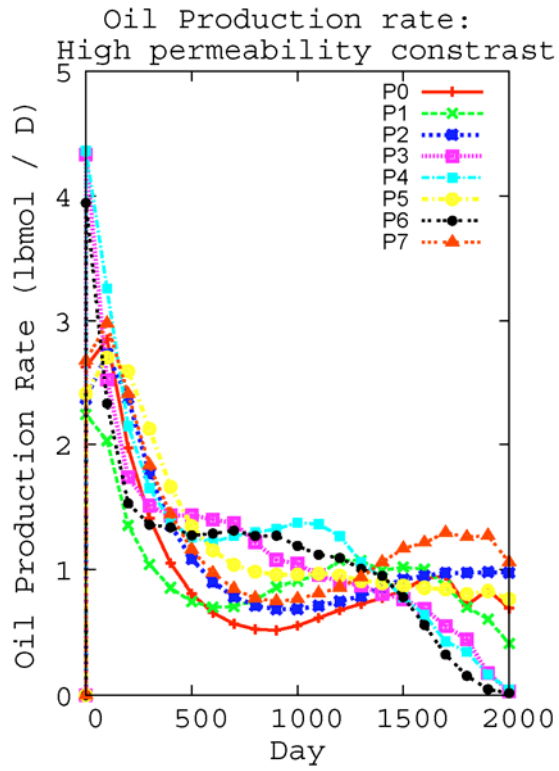

(b)

Figure 5: Oil production rate in steam flooding: a. Low permeability contrast; b. High permeability contrast

Figure 6: Domain of 1/4 five spot in-situ combustion simulation. Blue cylinder: production well, red cylinder: injection well.

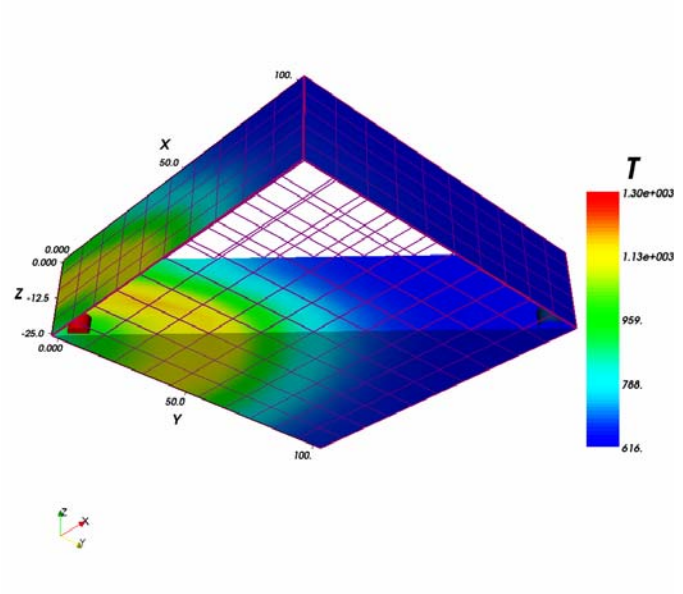

(a)

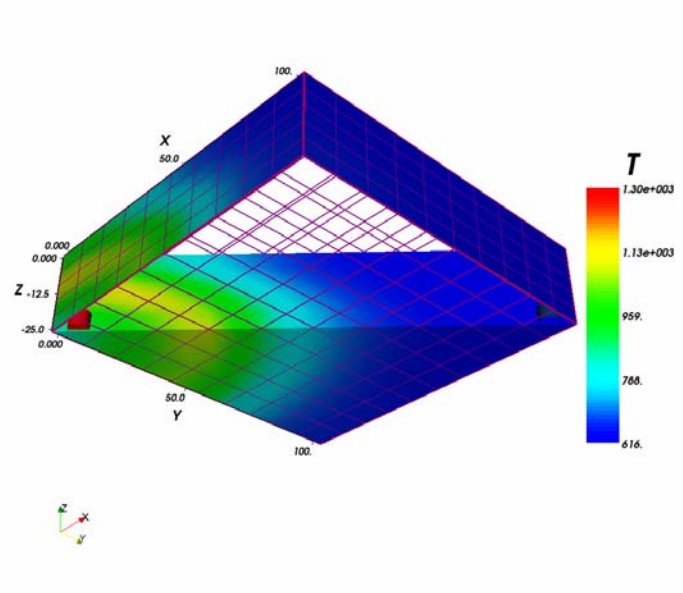

(b)

Figure 7: Temperature profiles in in-situ combustion (time = 40 days); a. Dry combustion; b. air to water ratio of 80:20

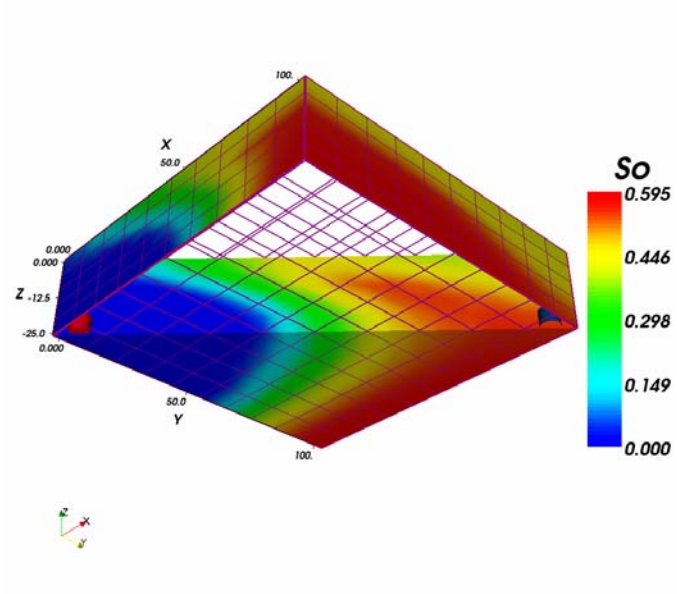

(a)

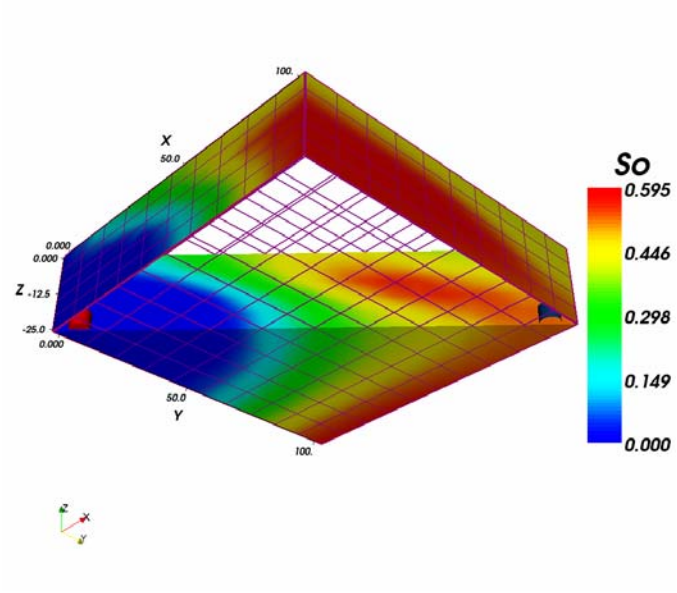

(b)

Figure 8: Oil saturation profiles in in-situ combustion (time = 40 days); a. Dry combustion; b. air to water ratio of 80:20

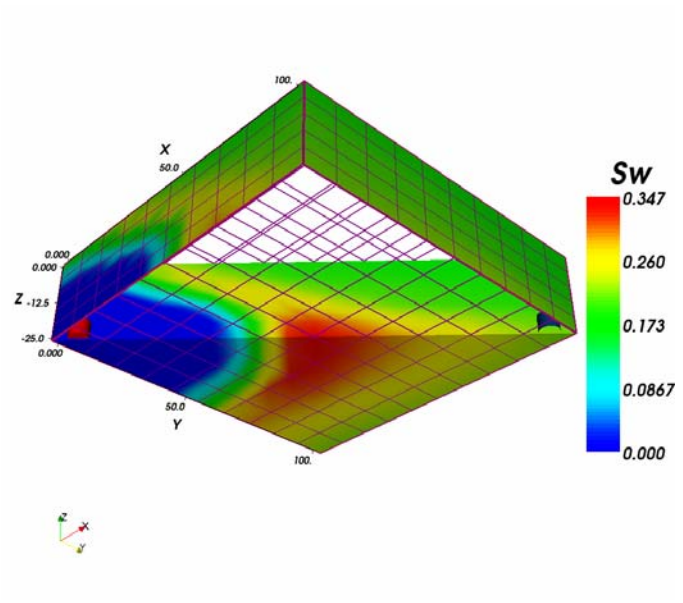

(a)

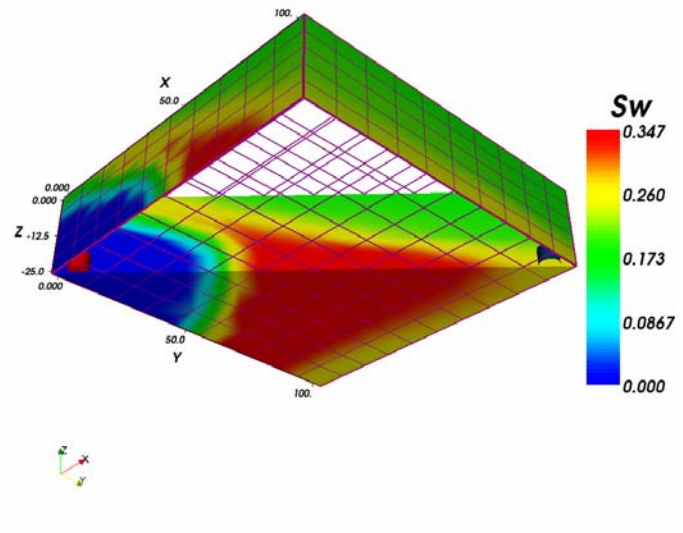

(b)

Figure 9: Water saturation profiles in in-situ combustion (time = 40 days); a. Dry combustion; b. air to water ratio of 80:20

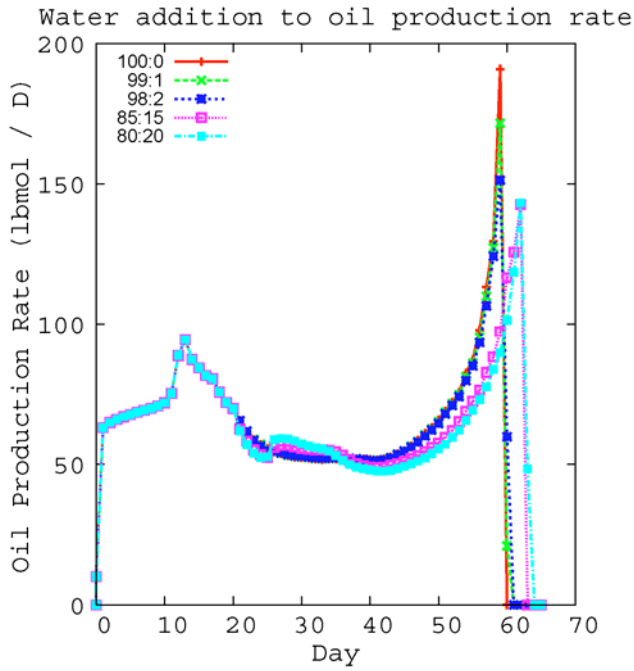

Figure 10: Oil production rate in in-situ combustion

Appendix

K-value equation in this thermal model is only a function of temperature and pressure. For a component 'i', the molar fraction in phases 'p1' and 'p2' can be computed by the following equation.

$$K_{i,p_L-p_H} = \frac{x_{p_L,i}}{x_{p_H,i}}$$

$$= \left(\frac{kv_0}{P} + kv_1 P + kv_2\right) \exp\left(\frac{kv_3}{T - kv_4}\right)$$

Pure component properties in each phase are computed first. Mixing rules are used to obtain the phase properties. Equations to compute molar density, viscosity and enthalpy for pure component are shown below

Molar density: [lbmol/ft^3]
liquid:

$$\rho = \frac{\rho^\circ}{\exp\left(c_{t_1}(T - T_0) + 0.5c_{t_2}(T^2 - T_0^2) - c_p(P - P_0)\right)}$$

solid:

$$\rho = \frac{\rho^\circ}{\exp\left(c_{t_1}(T - T_0) - c_{pt}(P - P_0)(T - T_0)\right)}$$

Viscosity: [cP]
liquid:

$$\mu = cl_0 \exp\left(\frac{cl_1}{T}\right)$$

$$\mu_w = cw_0 + cw_1 T \text{ (for water)}$$

gas:

$$\mu_g = cg_0 T^{cg_1}$$

Enthalpy: **[Btu/lbmol]**
liquid:

$$\bar{H} = \bar{H}^\circ_{IG} + \int_{T^\circ}^{T} <\bar{C}p_g> dT - \widehat{H}_{evp}(Tc - T)^{Ev}$$

gas:

$$\bar{H} = \bar{H}^\circ_{IG} + \int_{T^\circ}^{T} <\bar{C}p_g> dT$$

solid:

$$\bar{H} = \bar{H}^\circ_{s} + \int_{T^\circ}^{T} <\bar{C}p_s> dT$$

where

$$<\bar{C}p_p> = \bar{C}p_{p0} + \bar{C}p_{p1}T + \bar{C}p_{p2}T^2 + \bar{C}p_{p3}T^3 + \ldots$$

Phase properties such as molecular weight, molar density, pecific mass density, viscosity, enthalpy and internal energy are computed by using the following equations.

Molecular weight: [lb/lbmol]

$$M_p = \sum_{i=1}^{Nc} x_{p,i} M_i$$

Molar density:[lbmol / ft^3]

liquid:

$$\frac{1}{\rho_l} = \sum_{i=1}^{Nc} \frac{x_{l,i}}{\rho_{l,i}}$$

gas (Redlich KWong EOS):

$$\rho_g = \frac{P}{Z_g R_g T}$$

$$Z_g^3 - Z_g^2 + (A - B - B^2)Z_g - AB = 0$$

$$A = 0.42747 \frac{P}{T^2} \sum_{i=1}^{Nc} \left(x_{g,i} \frac{Tc_i^2 \alpha_i^{0.5}}{Pc_i^{0.5}}\right)^2$$

$$A = 0.08664 \frac{P}{T} \sum_{i=1}^{Nc} \left(x_{g,i} \frac{Tc_i}{Pc_i}\right)$$

solid: the same as liquid

Specific mass density: [lb$_f$ / ft^3]

$$\gamma_p = \rho_p M_p \frac{g}{g_c}$$

Viscosity: [cP]
liquid:

$$\ln \mu_l = \sum_{i=1}^{Nc} x_{l,i} \ln \mu_{l,i}$$

gas:

$$\mu_g = \frac{\sum_{i=1}^{Nc} x_{p,i} \sqrt{M_i}\, \mu_{g,i}}{\sum_{i=1}^{Nc} x_{p,i} \sqrt{M_i}}$$

Enthalpy: [Btu / lbmol]

$$\bar{H}_p = \sum_{i=1}^{Nc} x_{p,i} \bar{H}_{p,i}$$

Internal energy: [Btu / lbmol]

$$\bar{U}_p = \bar{H}_p - \frac{P}{\rho_p}$$

Rock (inert component of the reservoir) properties are computed as follow,

Internal energy: [Btu / ft^3]

$$\overline{U}_R = \overline{U}^\circ_R + (cr_{t_0} + cr_{t_1} T)(T - T_i)$$

Porosity:

$$\phi = \phi^\circ(1 + cr_p (P - P_0))$$

Rock-Fluid interaction properties such as capillary pressures and relative permeabilities are computed by RockFluid module. For a three-phase system (oil, water and gas), we have two capillary pressures: Pc_{og} and Pc_{ow}. In general, Pc_{og} is a function of S_g and Pc_{ow} is a function of S_w. The phase pressure therefore is computed by

$$P_P = P_0 + P_{cop}$$

The derivative of phase pressure is computed as

$$\frac{\partial P_p}{\partial v} = \frac{\partial P_0}{\partial v} + \sum_{p=1}^{Np} \frac{\partial P_{cop}}{\partial S_p} \frac{\partial S_p}{\partial v}$$

Stone II model is used [8] for relative permeability calculation. Look-up tables are used to obtain kr_w and kr_g, which are functions of S_w and S_g, respectively. Relative permeability of the oil phase is computed as

$$kr_o = kr_{ocw} \left\{ \left(\frac{kr_{ow}}{kr_{ocw}} + kr_w \right) \left(\frac{kr_{og}}{kr_{ocw}} + kr_g \right) - kr_w - kr_g \right\}$$

Power law rate expression is used to account for the generation and consumption of the components from chemical reactions. Stoichiometries of chemical reaction and rate expressions for each reaction are defined in the input file. In the application, the rate expression for any reaction should be simplified into the form

$$\Re_r = k_0 \exp\left(\frac{Ea}{R_h T}\right) \prod_{i=1}^{Nc} C_i^{ni}$$

Reaction rate for each reaction will be pre-factored by stoichiometry of the specified component and added to component's conservation equation.